Available online at www.sciencedirect.com

ScienceDirect

Developmental Biology 299 (2006) 582–593

DEVELOPMENTAL BIOLOGY

www.elsevier.com/locate/ydbio

Genomes & Developmental Control

Stereospecificity and PAX6 function direct *Hoxd4* neural enhancer activity along the antero-posterior axis

Christof Nolte [a,b,1,2], Mojgan Rastegar [a,2,3], Angel Amores [c], Maxime Bouchard [a,d], David Grote [a,d], Richard Maas [e], Erzsebet Nagy Kovacs [a], John Postlethwait [c], Isabel Rambaldi [a], Sheldon Rowan [e], Yi-Lin Yan [c], Feng Zhang [a,b,4], Mark Featherstone [a,b,d,f,*]

[a] *McGill Cancer Centre, McGill University, 3655 Promenade Sir-William-Osler, Montreal, QC, Canada H3G 1Y6*
[b] *Department of Medicine, McGill University, 3655 Promenade Sir-William-Osler, Montreal, QC, Canada H3G 1Y6*
[c] *Institute of Neuroscience, University of Oregon, Eugene, OR 97403, USA*
[d] *Department of Biochemistry, McGill University, 3655 Promenade Sir-William-Osler, Montreal, QC, Canada H3G 1Y6*
[e] *Division of Genetics, Department of Medicine, Brigham and Women's Hospital and Harvard, Medical School, New Research Building, Rm. 458H, 77, Avenue Louis Pasteur, Boston, MA 02115, USA*
[f] *Department of Oncology, McGill University, 3655 Promenade Sir-William-Osler, Montreal, QC, Canada H3G 1Y6*

Received for publication 24 June 2006; revised 16 August 2006; accepted 25 August 2006
Available online 30 August 2006

Abstract

The antero-posterior (AP) and dorso-ventral (DV) patterning of the neural tube is controlled in part by HOX and PAX transcription factors, respectively. We have reported on a neural enhancer of *Hoxd4* that directs expression in the CNS with the correct anterior border in the hindbrain. Comparison to the orthologous enhancer of zebrafish revealed seven conserved footprints including an obligatory retinoic acid response element (RARE), and adjacent sites D, E and F. Whereas enhancer function in the embryonic CNS is destroyed by separation of the RARE from sites D–E–F by a half turn of DNA, it is rescued by one full turn, suggesting stereospecific constraints between DNA-bound retinoid receptors and the factor(s) recognizing sites D–E–F. Alterations in the DV trajectory of the *Hoxd4* anterior expression border following mutation of site D or E implicated transcriptional regulators active across the DV axis. We show that PAX6 specifically binds sites D and E *in vitro*, and use chromatin immunoprecipitation to demonstrate recruitment of PAX6 to the *Hoxd4* neural enhancer in mouse embryos. *Hoxd4* expression throughout the CNS is reduced in *Pax6* mutant Sey^{Neu} animals on embryonic day 8. Additionally, stage-matched zebrafish embryos having decreased *pax6a* and/or *pax6b* activity display malformed rhombomere boundaries and an anteriorized *hoxd4a* expression border. These results reveal an evolutionarily conserved role for Pax6 in AP-restricted expression of vertebrate Hoxd4 orthologs.

Keywords: Hoxd4; Transcription; Neural enhancer; Hindbrain; Rhombomere; Retinoic acid; RARE; Stereospecificity; Hoxd4a; Pax6; Phylogenetic footprint; Evolution; Conservation; Mouse; Zebrafish; Anterior; Border; Antero-posterior; Dorso-ventral; Embryonic patterning; Transgenic; Knockdown

* Corresponding author. Current address: School of Biological Sciences, Nanyang Technological University, 60 Nanyang Drive, Singapore 637551 Singapore. Fax: +65 6791 3856.
E-mail address: msfeatherstone@ntu.edu.sg (M. Featherstone).
URL: http://genome.sbs.ntu.edu.sg/Staff/MSFeatherstone/index.php (M. Featherstone).
[1] Current address: Stowers Institute for Medical Research, 1000 E. 50th Street, Kansas City, MO 64110, USA.
[2] Co-first authors.
[3] Current address: Developmental Biology Program, Hospital for Sick Children, MaRS Centre, Toronto Medical Discovery Tower, 101 College St, Toronto, ON, Canada M5G 1L7.
[4] Current address: Howard Hughes Medical Institute, Department of Medicine, University of California San Diego, 9500 Gilman Drive, CMMW 345, La Jolla, CA 92093, USA.

0012-1606/$ - see front matter © 2006 Elsevier Inc. All rights reserved.
doi:10.1016/j.ydbio.2006.08.061

Introduction

Hox genes encode homeodomain-containing transcription factors that pattern the embryos of all animals (Featherstone, 2003). In taxa as diverged as flies and mammals, individual *Hox* genes are expressed in precise and characteristic spatio-temporal domains along the antero-posterior (AP) axis of the trunk, assigning positional identity across this dimension, and directing the subsequent morphogenesis of multiple tissues and organs (Hombria and Lovegrove, 2003; Krumlauf, 1994). Numerous studies have confirmed the importance of such restricted expression for normal development. The identification and characterization of those proximal and long-range enhancers controlling *Hox* expression have therefore attracted considerable attention (Deschamps and van Nes, 2005).

The 39 *Hox* genes of mice and humans are grouped at four discrete chromosomal loci designated the *HoxA* through *HoxD* clusters. The order of genes in each cluster is reflected in their sequential activation in time and space along the AP axis of the trunk, a process known as colinearity (Deschamps and van Nes, 2005). The four clusters are evolutionarily related and can be aligned to reveal 13 paralog groups. Two genes of paralog group 4, *Hoxb4* and *Hoxd4*, are expressed in the embryonic CNS with an anterior border at rhombomeres 6 and 7 (r6/7) in the hindbrain (Morrison et al., 1997). Enhancers of both neurectodermal and mesodermal expression are located 3′ of *Hoxb4* (Morrison et al., 1997). Within the 3′ neural enhancer, early expression is dependent on an RARE (Gould et al., 1998) that binds retinoid receptor heterodimers, whereas later expression is directed by a pararegulatory element recognized by HOXB4 and HOXD4 homeoproteins and capable of setting the correct r6/7 border (Gould et al., 1997). As for *Hox* genes in *Drosophila*, the maintenance of *Hoxb4* in a repressed state is controlled by chromatin modifying products of the Polycomb family (Suzuki et al., 2002).

These and other studies (Deschamps and van Nes, 2005; Gavalas and Krumlauf, 2000; Krumlauf, 1994) have established some of the major players at the DNA and protein levels acting through *Hox* neural enhancers. Nonetheless, the identified factors alone cannot account for all aspects of neural-specific *Hox* gene expression, and virtually nothing is known about how multiple transcriptional regulators act combinatorially to implement the precise spatio-temporal activation of diverse *Hox* enhancers. We have used mutational analysis in transgenic mouse embryos, coupled with phylogenetic footprinting with zebrafish *hoxd4a*, to identify *cis*-acting elements within the murine *Hoxd4* neural enhancer (Morrison et al., 1997; Nolte et al., 2003; Zhang et al., 1997, 2000). In addition to an RARE conserved in murine *Hoxb4* and zebrafish *hoxd4a*, we have noted six closely clustered footprints suggestive of functionally important transcription factor binding sites (Nolte et al., 2003). Once functions for such conserved elements are confirmed, a major challenge is to determine the specific transcription factors that recognize them, and how they cooperate with each other to set the correct *Hoxd4* expression domain.

Region-specific neural differentiation along the dorso-ventral (DV) axis of the neural tube is accomplished through the spatially restricted expression of three homeodomain-containing proteins: PAX3, PAX6, and NKX2.2 (Wilson and Maden, 2005). While *Pax3* is expressed most dorsally, *Pax6* transcripts occupy a broad medial domain in mid-gestational mouse embryos. Besides the DNA-binding homeodomain (HD), PAX3 and PAX6 harbor a so-called paired domain (PD), itself composed of two distinct DNA-binding structures (Chi and Epstein, 2002; Simpson and Price, 2002; Underhill, 2000). *Pax6* and its orthologs are master regulators of eye development throughout the animal kingdom, and *Pax6* mutation in humans and mice leads to ocular dysgenesis (Callaerts et al., 1997). In addition, *Pax6* mutant mice display malformations of the olfactory epithelium, pancreas, forebrain, hindbrain, and spinal cord, including altered motor neuron and interneuron identity in the latter two tissues (Ericson et al., 1997; Osumi et al., 1997).

Here, we further characterize the murine *Hoxd4* neural enhancer and show that three conserved elements directly adjacent to the RARE contribute to enhancer function in a stereospecific manner. PAX6 binds two of these elements *in vitro*, and is recruited to the enhancer in mouse embryonic trunk where *Hoxd4* is active, but not in cells of the head that do not express *Hoxd4*. Loss of *Pax6* decreases *Hoxd4* expression in the early mouse neural tube, consistent with broader AP and DV activation of *Pax6* at early developmental times. Confirming the evolutionary conservation of PAX6 function in Hoxd4 neural expression, reduced *pax6* activity in somite-matched zebrafish embryos alters rhombomeric boundaries and anteriorizes the *hoxd4a* expression border. Our results reveal a role for Pax6 in AP-restricted Hox gene expression, and suggest that stereospecific interactions between PAX6 and adjacently bound retinoid receptors may be important for *Hoxd4* neural enhancer function.

Materials and methods

Transgene constructs

Mutations of the mouse neural enhancer were generated by PCR overlap extension (Ho et al., 1989). The PCR primers used to generate construct 3 were (sense) 5′-TTTCTGTTCGCCCCGCTGTA-3′, (antisense) 5′-TACAGCGGGGCGAACAGAAA-3′; construct 4 (sense) 5′-TGTACCGCGGCCTGGAGGACTGACCTC-3′, (antisense) 5′-CAGGCCGCGGTACAGCTAATCGAACAG-3′; construct 5 (sense) 5′-CAGAATCACCCCCGGTTCACCCAGAGGACA-3′, (antisense)5′-TGTCCTCTGGGTGAACCGGGGGTGATTCTG-3′; construct 6 (sense) 5′-AGGACACCCCCAATTTTCTGTTCG-3′, (antisense) 5′-CGAACAGAAAATTGGGGGTGTCCT-3′; construct 7 (sense) 5′-AGGACACCCCCAAAGGGAATTTTCTGTTCG-3′, (antisense) 5′-CGAACAGAAAATTCCCTTTGGGGGTGTCCT-3′; construct 8 (sense) 5′-TTTCGTTCCCCCCGATTAG-3′, (antisense) 5′-CTAATCGGGGGGAACAGAAA-3′; construct 9 (sense) 5′-GTTCGATTACCCCCGCTGTA-3′, (antisense) 5′-TACAGCGGGGGTAATCGAAC-3′. These constructs were cloned into pSHlacZpA (Zhang et al., 2000). All clones were confirmed by manual sequencing.

Production of transgenic mice

The preparation and microinjection of the transgenes have been previously described (Nolte et al., 2003). Fertilized donor eggs were obtained from CBA × C57Bl6/J F1 mice bred in house. Microinjected embryos were implanted into CD1 (Harlan) pseudopregnant fosters.

Collection of embryos for genotyping, β-galactosidase staining, whole-mount in situ hybridization, and cryostat sectioning

Embryo collection, staining, and genotyping have been previously described (Nolte et al., 2003). Genotyping of SeyNeu embryos was performed as described (Hill et al., 1991; Xu et al., 1997) on extraembryonic membranes or on the embryos themselves following staining and photography. For whole-mount *in situ* hybridization, embryos were dissected and processed with digoxigenin-UTP-labeled RNA probes as described earlier (Henrique et al., 1995). *Hoxd4* expression was detected with the probe BgH (Folberg et al., 1997) which is complementary to the 3′ end of *Hoxd4* region, and detects all *Hoxd4* transcripts. Embryos presented in any given panel of Fig. 6 were collected at the same time and stained in the same experiment. In the case of Fig. 6C, the embryos were also stained in the same well followed by genotyping on the whole embryos. For the cryosectioning, embryos were embedded in OCT and 20 μm sections were collected on a Leica cryostat.

Production and analysis of zebrafish embryos having reduced pax6 function

Morpholino antisense oligonucleotides (MO) were obtained from Gene Tools (Philomath, OR), and were injected as described (Draper et al., 2001). In situ hybridization was performed as described (Jowett and Yan, 1996). The sequence of the MOs was as follows: *pax6a*, 5′-TTTGTATCCTCGCYGAAGTTCTTCG-3′ and *pax6b*, 5′-CTGAGCCCTTCCGAGCAAAACAGTG-3′. Probes used for detection of *eng2b*, *krox20a*, and *hoxd4a* have been previously described (Ekker et al., 1992; Oxtoby and Jowett, 1993; Prince et al., 1998). The *pax6a* probe was a gift from the Westerfield laboratory (Püschel et al., 1992), and the *pax6b* probe was obtained from ZIRC (cb566).

ChIP and real-time PCR

Chromatin immunoprecipitation (ChIP) experiments were performed as described previously (Rastegar et al., 2004). For ChIP with P19 cells, we used 10^6 cells per immunoprecipitation. Briefly, the cells were cross-linked with 1% formaldehyde, collected, and washed twice with ice-cold PBS containing protease inhibitor cocktail from Roche (complete EDTA-free). The cells were resuspended in 200 μl of sodium dodecyl sulfate (SDS) lysis buffer on ice for 10 min and then sonicated with 10 sets of 10-s pulses by a Betatec Sonics Vibra Cell sonicator to an average DNA size of 600 bp. ChIP experiments with embryonic tissues were done as described (Rastegar et al., 2004). E8.0 and E10.5 embryos were cross-linked with 1% formaldehyde diluted in serum-free Dulbecco's modified Eagle's medium (DMEM) for 15 min at room temperature. The cross-linked embryos were washed three times with PBS containing protease inhibitors for 10 min at room temperature. The E8.0 embryos were dissected into anterior (head) and posterior (trunk) regions, as described before (Rastegar et al., 2004). The E10.5 embryos were mildly digested with 0.5% trypsin in Ca^{2+}-free DMEM containing 20 mM HEPES for 25 min at 4°C in order to finely dissect the neural tube from the developing somites and other embryonic tissues. After a wash step with Ca^{2+}-containing DMEM, fine forceps were used to separate the neural tube from the neighboring tissue under a dissecting microscope. A section was then made with a razor blade at the base of the otic vesicle, parallel to the r6/7 boundary, separating spinal cord tissue from the head. The cells (10^6) were lysed for 15 min on ice in 1 ml of cell lysis buffer [5 mM piperazine-*N*,*N*′-*bis*(2-ethanesulfonic acid) (PIPES; pH 8.0), 85 mM KCl, 0.5% NP-40], pelleted, and incubated with 200 μl of SDS lysis buffer for an additional 20 min on ice to release the chromatin. Chromatin samples were then sonicated and processed further as for P19 cells. The chromatin was precleared with salmon sperm DNA–protein A–agarose beads for 1 h, followed by an overnight incubation with different antibodies. For each experiment with P19 cells, we used 5 μl of anti-PAX6-C-terminal antibody (Turque et al., 1994) per half million cells. Chromatin–antibody complexes were collected by reincubation for 1 h with protein A–agarose beads. Washes were performed according to the Upstate protocol. Chromatin was eluted from the beads and cross-links were reversed at 65°C for 4 h. DNA was phenol–chloroform extracted and ethanol precipitated. Five percent (by volume) of the immunoprecipitated material was used as a template for real-time PCR by use of a SYBR Green Taq ReadyMix kit for quantitative PCR from Sigma and a Roche LightCycler. PCR products were run in 1.5% agarose gels and visualized by ethidium bromide staining. Quantification of the LightCycler data measured the relative amounts of initial target sequence and expressed them as a percentage of the input. Standard curves of serially diluted target sequences were used for quantification.

Primers

The sequence of primers used for ChIP of the *Hoxd4* enhancer and *gapdh* control has already been published (Rastegar et al., 2004). The primers used for the bandshift experiments were as follows:

RARE-D–E:
5′-ATCAGGTTCACCCAGAGGACAAATTTTCTGTTCGATTAGCTGT-3′
5′-ACAGCTAATCGAACAGAAAATTTGTCCTCTGGGTGAACCTGAT-3′
D-E:
5′-ACAAATTTTCTGTTCGATTAGCTGTATTT-3′
5′-AAATACAGCTAATCGAACAGAAAATTTGT-3′
D:
5′-GAGGACAAATTTTCTGTTCGAT-3′
5′-ATCGAACAGAAAATTTGTCCTC-3′
E:
5′-GAGGACAACCCGCGGATTCGATTAGCTGTATTT-3′
5′-AAATACAGCTAATCGAATCCGCGGGTTGTCCTC-3′
P3: paired homeodomain binding site (Wilson et al., 1995):
5′-GGGAATAATCTGATTACAGGG-3′
5′-CCCTGTAATCAGATTATTCCC-3′
PAX6CON: PAX6 PD consensus binding site (Epstein et al., 1994)
5′-GCAAATTTTCACGCTTGAGTTCACAGCT-3′
5′-AGCTGTGAACTCAAGCGTGAAAATTTGC-3′
5C's between RARE and site D:
5′-ATCAGGTTCACCCAGAGGACACCCCCAATTTTCTGTTCGATTAGCTGT-3′
5′-ACAGCTAATCGAACAGAAAATTGGGGGTGTCCTCTGGGTGAACCTGAT-3′
5C's between site D and E:
5′-ATCAGGTTCACCCAGAGGACAAATTTTCTGTTCCCCCCGATTAGCTGT-3′
5′-ACAGCTAATCGGGGGGAACAGAAAATTTGTCCTCTGGGTGAACCTGAT-3′

Total cell extracts and immunoblotting

Total P19 cell extracts or embryonic cell extracts were prepared as described previously (Rastegar et al., 2004). Twenty-microgram samples of total cell extracts were run in SDS-10% polyacrylamide gels and transferred to nitrocellulose membranes. The membranes were blocked for 1 h at room temperature in 5% nonfat milk powder and 0.1% Tween 20 in PBS (PBS-T). Incubation with the primary antibody was performed either for 2 h at room temperature or overnight at 4°C, and the membranes were subsequently washed in 0.1% PBS-T. Incubation with a horseradish peroxidase-conjugated secondary antibody was done for 45 min at room temperature, followed by washing with 0.1% PBS-T. Bound immunoglobulins were visualized with an enhanced chemiluminescence detection system (Mandel Biotech). The membranes were then stripped and reprobed with an anti-actin antibody as a loading control.

Antibodies

The anti-PAX6 C-terminal antibody and the anti-PAX6 paired domain antibody (Turque et al., 1994) are kind gifts of Dr. Simon Saule. The anti-actin AC40 antibody was purchased from Sigma.

Immunohistochemistry

The protocol for immunohistochemistry on sectioned embryos (Haller et al., 2002; Hogan et al., 1994), and for embryo fixation and sectioning (Daniels et al., 1996) were as described.

In vitro transcription-translation and electrophoretic mobility shift assay

PAX6 protein was generated with an Sp6 TNT coupled *in vitro* transcription-translation kit (Promega). Reactions containing [^{35}S] methionine were performed in parallel to verify translational efficiency. Electrophoretic mobility shift assay (EMSA) was performed as described previously (Phelan et al., 1995).

Results

The sequence and spacing of conserved elements direct Hoxd4 neural enhancer activity

We have shown that the zebrafish *hoxd4a* gene bears an orthologous neural enhancer conserved in position, sequence and function with its murine ortholog (Zhang et al., 2000). Phylogenetic footprints A through F obtained by sequence comparison of the zebrafish and mouse enhancers are likewise conserved in human and chicken (Fig. 1A). Our previous work showed that a 3′ deletion of the murine *Hoxd4* neural enhancer removing sites D, E and F (Fig. 1A) abolishes CNS expression in transgenic mouse embryos (Zhang et al., 2000). To understand the contribution of each individual site to enhancer function, we used site-directed mutagenesis in the same reporter context and tested the mutants in transient transgenic analysis (Fig. 1B). As reported previously (Zhang et al., 2000), mutation of site D results in a posteriorization of the anterior border (construct 2, Figs. 2, 3C). We examined this mutant in greater detail by making flatmounts of the hindbrain region which more clearly reveal the extent of posteriorization (Fig. 3G). The anterior expression border of site D mutants is ragged and retracted, with greater posteriorization in the ventral aspect. Mutation of site E gave a similar result, although the discrepancy between ventral and dorsal aspects was more pronounced (construct 3, Figs. 2, 3D, H). Mutating site F produced more subtle effects, with a slight posteriorization evident on the left side of the embryo shown, in addition to variable cell-to-cell expression in the dorsal aspect (construct 4, Figs. 2, 3E, I).

The above results show that neural enhancer activity is posteriorized by individual mutation of sites D, E, and F. However, simultaneous deletion of all three sites abolishes enhancer function (Zhang et al., 2000). This suggests that these sites make synergistic contributions to the overall strength of neural expression. We noted that the spacing between the RARE and site D (3 bp), and between sites D and E (2 bp) is evolutionarily conserved (Fig. 1B), suggesting that factors bounds to these elements may physically interact in a spatially constrained manner. To test for such stereospecific interactions, we introduced 5-bp insertions between the various sites in the *Hoxd4* neural enhancer, thereby displacing factors bound on either side of the insertion by 180° around the DNA double helix. When placed between site C and the RARE, a 5-bp insertion had no effect on transgene expression (construct 5, Figs. 2, 3J, O). However, when the insertion was located between the RARE and site D, *lacZ* expression in the neural tube was largely eliminated (construct 6, Figs. 2, 3K, P). Thus, separating sites D, E and F from the RARE by 5 bp is as deleterious as removal of these sites entirely, and more crippling than mutation of D, E or F individually.

To assess the spacing requirements of individual elements, we introduced 5 bp between sites D and E (construct 8, Figs. 2, 3M, R), or E and F (construct 9, Figs. 2, 3N, S). The insertion between sites D and E resulted in a posteriorization, but not elimination, of transgene expression, similar to mutation of site D. Although the distance between sites E and F is not conserved between mice and fish, the introduction of five cytosines anteriorized transgene expression toward the r5/6 border. In all embryos expressing this construct, ectopic expression in the head was also greatly enhanced. Thus, only insertion between the RARE and site D mimicked deletion of all three sites D, E and F by abolishing enhancer activity.

If a 180° displacement of the RARE from sites D–E–F disrupts stereospecific interactions between adjacently bound factors, then realignment by insertion of six additional nucleotides (one full turn) should rescue neural expression. Such a construct bearing an 11-bp insertion between the

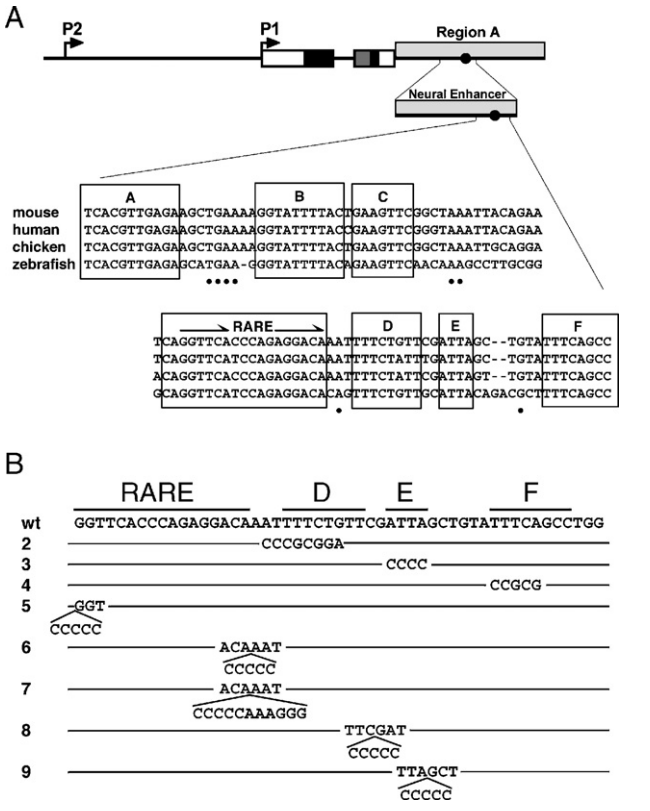

Fig. 1. (A) Diagram of the *Hoxd4* transcription unit contained in the pSNlacZpA transgene showing downstream (P1) and upstream (P2) promoters, non-coding (white boxes) and coding exons (black boxes), homeobox (dark grey box), the 3′ region containing neural and mesodermal enhancers (light grey, region A), the minimal neural enhancer, the position of the RARE (black circle) and a sequence comparison of the most highly conserved neural enhancer elements shared by mouse, human, chicken and zebrafish (RARE plus sites A through D). The half sites in the RARE are given by overlying half-arrows. Dashes are placed opposite base pair insertions. (B) Mutations introduced in the region spanning the RARE and sites D, E and F. Construct number is given at the left. Base substitutions are given directly below the corresponding wild-type sequence. Sites of 5- or 11-bp insertions are given along with the 6-bp spanning the insertion site.

RARE and site D was indeed active throughout the majority of the *Hoxd4* neural expression domain (construct 7, Figs. 2, 3L, Q), though not in anterior-most cells adjacent to the r6/7 border. We conclude that stereospecific interactions between retinoid receptors and factor(s) bound to at least site D are critical for *Hoxd4* neural enhancer function.

PAX6 is recruited to the Hoxd4 neural enhancer in vitro and in vivo

Mutations involving sites D or E (constructs 2, 3 and 8) differentially affected transgene expression along the neural D–V axis, suggesting the involvement of transcriptional regulators directing D–V patterning. PAX3 and PAX6 are two such factors (Wilson and Maden, 2005). Moreover, *Pax6* is expressed in the hindbrain and throughout the neural tube as early as E8.0 (Walther and Gruss, 1991), a few hours before the onset of *Hoxd4* expression (Featherstone et al., 1988; Gaunt et al., 1989). Inspection of the sequence spanning sites D and E revealed moderate identity with PAX6CON (Epstein et al., 1994), the consensus binding site for the PAX6 PD (Fig. 4A). Given that many naturally occurring PAX6 binding sites are poorly related to the consensus (Fig. 4A) (Cvekl et al., 1994, 1995), we produced PAX6 in rabbit reticulocyte lysates and tested by EMSA for specific binding to a double-stranded oligonucleotide probe spanning the RARE and sites D and E. Unprogrammed lysate gave several bands, some of which were due to endogenous rabbit PAX6 (Supplemental Fig. 1). Programmed lysate expressing murine PAX6 gave an additional DNA-bound complex that was specifically competed by

Construct		# express/ total Tg	r6/7 border	description
1		9/9	7/9	wild type
2		5/7	0/7	posteriorized
3		3/5	0/5	posteriorized
4		10/13	10/13	ventral edge posteriorized
5		3/7	3/7	wild type
6		5/10	0/10	abolished
7	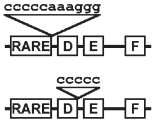	7/11	0/11	rescued, posteriorized
8	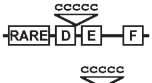	6/10	0/10	posteriorized
9	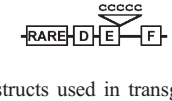	4/4	0/4	anteriorized

Fig. 2. Constructs used in transgenic analysis of the *Hoxd4* neural enhancer. Mutation of sites D, E, and F are indicated by a cross through the corresponding site. Half- and full-helical insertions are shown with inverted triangles above the point of insertion. #Express/total Tg: the fraction of embryos expressing the construct over the total number of transgenics as determined by PCR on yolk sac material. r6/7 border: the number of embryos displaying the correct r6/7 anterior expression border over the total number of transgenics. Numbers for construct 1 are taken from (Zhang et al., 2000).

PAX6CON (Epstein et al., 1994), but not by the PAX HD binding site P3 (Wilson et al., 1995) (Fig. 4B) or non-specific oligonucleotides (data not shown). These implicate the PAX6 PD in binding to the *Hoxd4* neural enhancer, and suggest that the HD plays at most an indirect role.

Confirmation that the shifted band was indeed due to PAX6 binding was obtained with specific antibodies. Two polyclonal antibodies directed against the PAX6 HD or C-terminus (Turque et al., 1994) supershifted the presumptive PAX6 complex (Fig. 4C), whereas a control polyclonal antibody against murine HOXD4 did not (data not shown). Likewise, complexes formed on the same site with lysates of neurally differentiating P19 cells or extracts of E10.5 embryonic spinal cord were super-shifted by PAX6 antibody (data not shown).

To refine the region bound by PAX6, cold competitors corresponding to sites D–E, D only, and E only, were used with the RARE-D–E probe. While the D–E probe efficiently competed PAX6 binding, neither of sites D or E alone were effective competitors (Fig. 4D). We used competitor oligonucleotides to test PAX6 binding to two 5-bp spacing mutants used in transgenic analysis. Five-bp insertions between the RARE and site D, or between sites D and E, were both effective competitors in EMSA (Fig. 4D), suggesting that altered expression seen with each mutant is not due to decreased intrinsic affinity for PAX6 alone. Last, we confirmed that a labeled probe containing sites D and E but not the RARE was directly bound by PAX6 (Fig. 4E). These results implicate both sites D and E in the binding of the PAX6 PD, consistent with the homology of D–E with the PAX6 PD consensus binding site, and the placement of D and E at positions predicted to contact the PD N- and C-subdomains, respectively (Fig. 4A) (Xu et al., 1999). They also reveal a possible tolerance by the PAX6 PD for recognition of separated sites for N- and C-subdomain binding.

The ChIP assay was used to study PAX6 binding to the *Hoxd4* neural enhancer *in vivo*. The *Hoxd4* gene is inactive in undifferentiated P19 EC cells, but is induced within 2 days following neural induction by RA. Induction is accompanied by chromatin modification and transcription factor recruitment to the enhancer (Rastegar et al., 2004). ChIP assays performed on chromatin from P19 cells revealed recruitment of PAX6 to the *Hoxd4* neural enhancer specifically during neural induction (Fig. 5A). Although PAX6 is present in P19 before neural differentiation, it is not found at the enhancer, consistent with specific recruitment during the activation of *Hoxd4*.

We have previously shown that chromatin modification and transcription factor recruitment at the *Hoxd4* enhancer have already commenced on early day 8 specifically in the trunk neural tube where *Hoxd4* will be expressed a few hours later. By contrast, these changes do not take place in the head region where *Hoxd4* remains inactive (Rastegar et al., 2004). ChIP assays on chromatin from dissected regions of E8.0 embryos reveal PAX6 recruitment to the *Hoxd4* neural enhancer only in the trunk and not the head, thus anticipating gene activation in the trunk at E8.25 (Figs. 5A, B). By E10.5, however, PAX6 is no longer associated with the enhancer, though *Hoxd4* remains

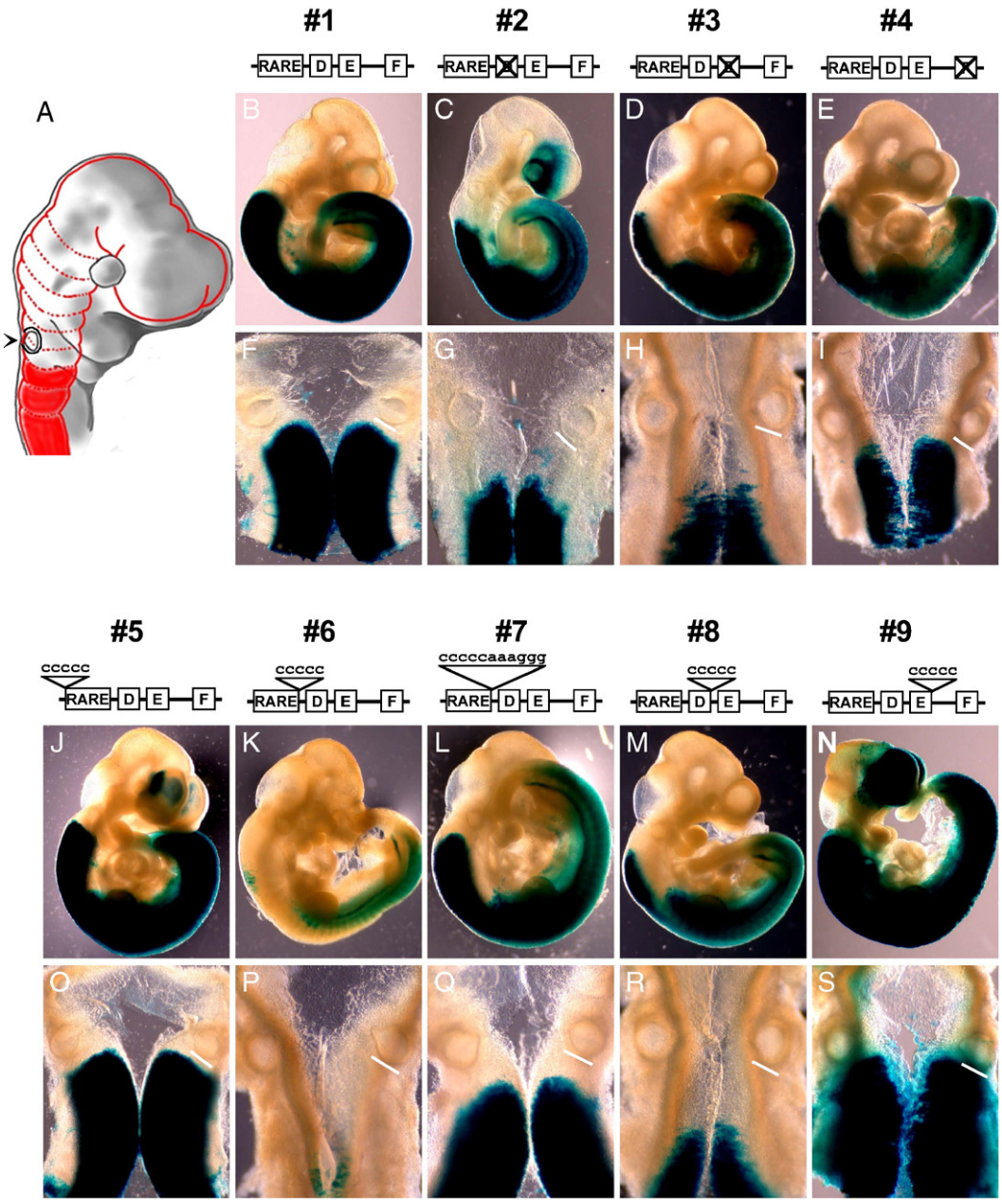

Fig. 3. Binding site or insertional mutations alter the setting of the anterior neural expression border of *Hoxd4* transgenes. (A) Cartoon of E9.5 embryo with the CNS outlined in continuous red lines and the boundaries between rhombomeres denoted by dashed red lines. The *Hoxd4* expression domain with the r6/7 expression boundary is given by solid red fill. The posterior border of the otic vesicle (arrow head) lies just anterior to the r6/7 border. (B–S) Lateral and flatmount views of transgenic embryos. Construct numbers and pictorials are given on top of each pair of photographs. The posterior edge of the otic vesicle (right side) is given by a solid white line.

actively transcribed (Fig. 5B). Together, these results demonstrate specific association of PAX6 with the *Hoxd4* neural enhancer.

Hoxd4 neural enhancer activity is dependent on PAX6

Pax6 expression is excluded from the most dorsal and ventral regions of the neural tube in mid-gestational mouse embryos (Wilson and Maden, 2005), raising questions as to how it could influence *Hoxd4* expression across the entire D–V axis. We assessed to what extent *Hoxd4* and *Pax6* are co-expressed in the early neural tube by examining the distribution of *Hoxd4* transcripts and PAX6 protein along the DV axis of the posterior rhombencephalon at E8.5. Immunohistochemistry with a polyclonal PAX6 antibody (Turque et al., 1994) revealed broad distribution across the D–V axis of the posterior hindbrain (Fig. 6B) that is largely coextensive with *Hoxd4* transcripts (Fig. 6A). Thus, early PAX6 expression shows less DV restriction than at later stages, consistent with observations in chick (Ericson et al., 1997), and providing for a direct role in regulating *Hoxd4* throughout this axis in the neural tube.

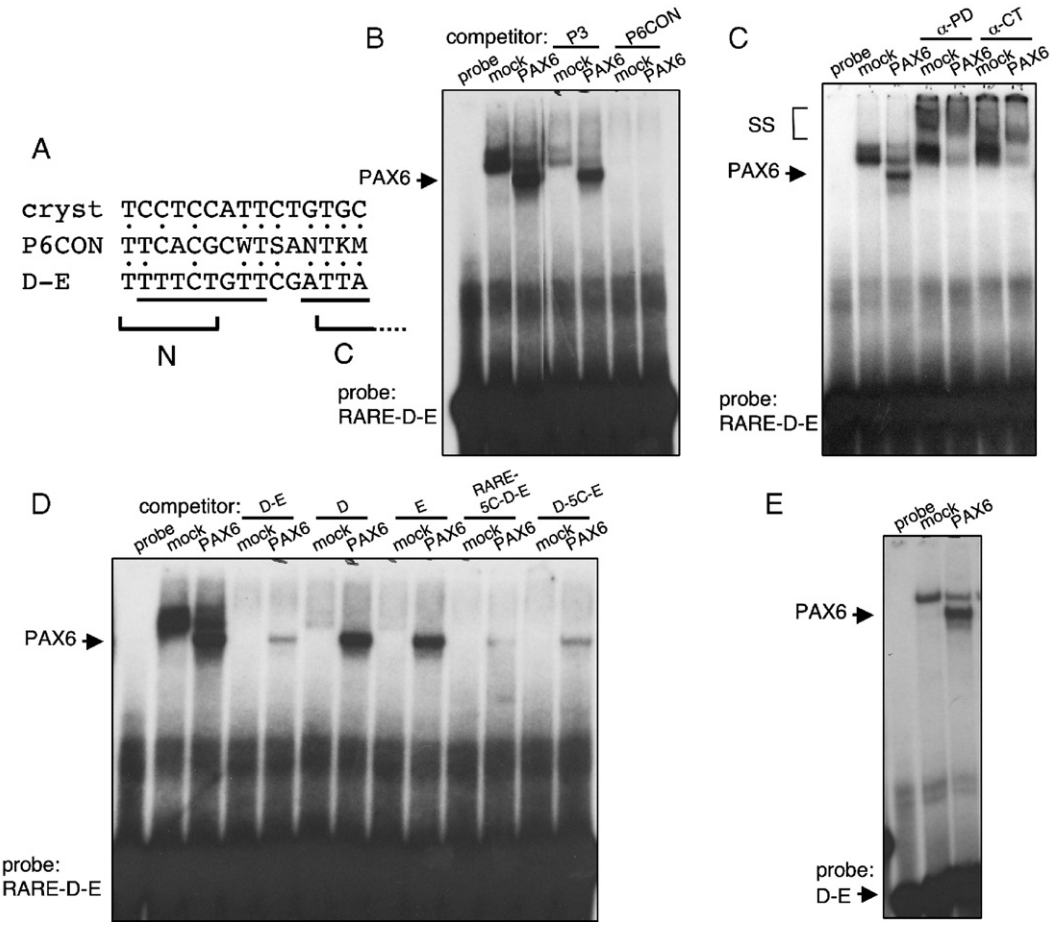

Fig. 4. PAX6 binds sites D and E *via* the paired domain. (A) Comparison of the consensus PAX6 PD binding site PAX6CON (P6CON) with the sequence of *Hoxd4* D–E (below) and the PAX6 binding site of the αA-crystallin gene (cryst) (Cvekl et al., 1995). Base pair identity shown by dots. Sites D and E are underlined, and the regions predicted to contact the N- and C-subdomains of the PD are bracketed (Xu et al., 1999). (B–E) EMSA analysis of PAX6 binding to the *Hoxd4* neural enhancer. Position of specific PAX6-DNA complexes, of supershifted complexes (SS), and probe and probe identity, are given at the left of each panel. The protein used in each reaction is given at the top of each lane. Competitors and antibodies are indicated above horizontal lines top-most in each panel. Probe, free probe. The prominent shifted complex in the "mock" lane is due to the presence of endogenous PAX6 in rabbit reticulocyte lysates as shown by controls in EMSA and Western blot analysis (Supplemental Fig. 1). Mock, unprogrammed reticulocyte lysate. PAX6, *in vitro* translated murine PAX6. αPD, antibody against PAX6 PD. αCT, antibody against PAX6 C-terminus. P3, competitor harboring the consensus PAX HD binding site. P6CON, competitor harboring the consensus PAX6 PD binding site PAX6CON. (B) PAX6 binds to an oligonucleotide spanning the RARE and sites D and E of the *Hoxd4* neural enhancer. Binding is dependent on the PD but not the HD, as evidenced by competition with the PD binding site PAX6CON (P6CON) but not the HD binding site P3. The panel has been digitally spliced between the third and fourth lanes. (C) The presumptive PAX6 complex is supershifted by antibodies against the PAX6 PD and C-terminus. (D) PAX6 binding is dependent on both sites D and E, and is not disrupted by a 5-bp insertion between D and E. (E) A binding site containing only sites D and E is sufficient to recruit PAX6.

To test directly the role of Pax6 in regulating Hoxd4 expression in the vertebrate embryo, we assessed gene activity in two developmental contexts: first, in mouse embryos homozygous for a *Pax6* null mutation, and second, in zebrafish embryos having reduced pax6 co-ortholog function following transcript knockdown with morpholino oligonucleotides. *Hoxd4* transcript distribution was examined in the Sey^{Neu} mouse strain. The Sey^{Neu} strain of *Pax6* mutants arose from a chemically treated stock, and bears a point mutation in a splice donor site that effectively truncates the resulting protein after the HD, thereby deleting the C-terminal transactivation domain (Hill et al., 1991). Sey^{Neu} heterozygotes present olfactory and ocular malformations typical of *Pax6* mutants, while homozygotes die at birth (Callaerts et al., 1997). *Hoxd4* expression in stage-matched embryos from matings of Sey^{Neu} heterozygotes was assessed by whole-mount *in situ* hybridization. Wild-type and Sey^{Neu} heterozygotes displayed near-equivalent levels of *Hoxd4* expression in the neuroectoderm. Of the four homozygous Sey^{Neu} embryos obtained, two could be matched by somite number to wild-type and heterozygous littermates (Fig. 6). Sey^{Neu} homozygotes revealed markedly decreased expression throughout the neural tube at E8.5 (10 to 11 somites, Fig. 6C) and E8.75 (13 to 14 somites, Figs. 6E–F). The remaining two homozygotes likewise showed decreased *Hoxd4* expression, but were developmentally delayed by one somite (data not shown). By E11.0, wild-type *Hoxd4* expression levels are restored in the CNS of Sey^{Neu} homozygotes (data not shown), suggesting independent regulatory mechanisms at later developmental stages.

The zebrafish genome has but a single Hoxd4 ortholog, *hoxd4a*. The combined expression patterns of the two zebrafish Pax6, *pax6a* and *pax6b*, comprise the entire hindbrain field (Supplemental Fig. 2) and therefore fully

overlap the *hoxd4a* expression domain in this tissue. To address the role of *pax6a* and *pax6b* in *hoxd4a* expression, one-cell stage embryos were injected with morpholino antisense oligonucleotides (MOs) for *pax6a* and/or *pax6b*, and messages for *eng2b*, *krox20a*, and *hoxd4a* were detected by whole-mount *in situ* hybridization. Decreased expression of the PAX6 target gene *eng2b* at the midbrain–hindbrain border confirmed that the MOs had indeed engendered *pax6a* and *pax6b* loss-of-function (Fig. 7). By comparison to control-injected, somite-matched embryos (14 and 16 somites), the expression patterns for *krox20a* and *hoxd4a* revealed developmental perturbations to hindbrain patterning. Dorsal views of both 14-somite (Figs. 7A–D) and 16-somite embryos (Supplemental Fig. 3) show a decrease in the gap separating the *krox20a* expression domain in r5 from the anterior domain of *hoxd4a* expression in r7. Lateral views of 14-somite embryos provided more detailed information (Figs. 7E–H). Strikingly, the AP widths of r5 and r6 were contracted ventrally relative to control-injected embryos, and were accompanied by anteriorization of the *hoxd4a* expression

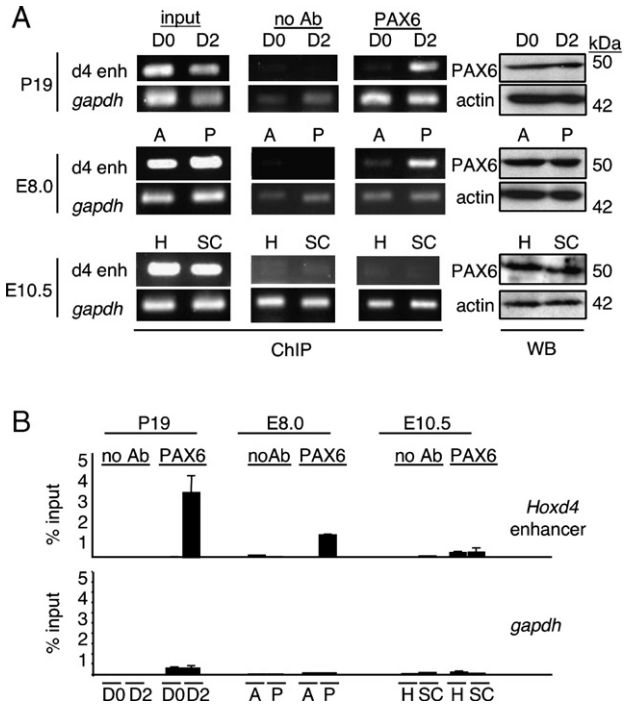

Fig. 5. PAX6 is recruited to the *Hoxd4* neural enhancer *in vivo*. (A) Results of ChIP and Western blot (WB) analyses, as indicated below the panels. One set of assays was performed on P19 cells at the beginning (day 0, D0) and 2 days following (D2) the onset of neural differentiation (top panels). *Hoxd4* expression is turned on at D2. Remaining assays used tissue extracts of E8.0 anterior (A) and trunk (P), and E10.5 head (H) and spinal cord (SC). d4 enh, amplification of the *Hoxd4* neural enhancer. *gapdh*, amplification of a genomic region of a *gapdh* control. PCR was performed on unprecipitated chromatin (input), mock precipitated without antibody (no Ab), and anti-PAX6 antibody. Western blots were probed with antibodies against PAX6 or actin, as indicated. Molecular mass (kDa) for both species is given at right. Western blots show that differences in PAX6 recruitment are not due to global changes in PAX6 levels in the cell. (B) ChIP results from the LightCycler were quantitated and expressed as percent input. Error bars show the SEM from at least two independent experiments.

border in its more ventral aspects. This phenotype was most prominent in embryos injected with both *pax6a* and *pax6b* MOs (Fig. 7H). In fact, AP patterning defects were detected in virtually all rhombomeres 1 through 7. These phenotypes were seen in 98 of 110 (*pax6a* MO), 83 of 85 (*pax6b* MO), and 95 of 102 (*pax6a*+*pax6b* MOs) injected embryos. Combined with the overall lower expression levels of *hoxd4a* in the experimentally injected embryos, these results confirm a role for Pax6 in setting both the anterior border and strength of Hoxd4 expression in vertebrate embryos.

Discussion

Sequence and spacing requirements at the Hoxd4 neural enhancer

Phylogenetic footprinting (Tagle et al., 1988) assumes a strong evolutionary selection against base substitution within transcription factor binding sites but not in surrounding sequences. Sequence conservation has been used successfully in the past to identify *cis*-acting regulatory elements in *Hox* enhancers (Gould et al., 1997), and our own previous work revealed seven such footprints in a conserved core within the neural enhancers of mouse and zebrafish Hoxd4 orthologs (Nolte et al., 2003). Our present and previous studies show that all four footprints examined to date (RARE, D, E and F) do indeed contribute to *Hoxd4* enhancer function.

Our results further show that the insights of this method are acquired not only through sequence conservation, but also through evolutionary conservation of spacing between footprints. We used the standard tests for stereospecific interactions on DNA by insertion of 5 or 11 bp, corresponding to one half turn and one full turn of the helix, respectively (Takahashi et al., 1986). Five-bp insertions between RARE-D, D–E and E–F all displaced transgene expression from the correct r6/7 boundary in the hindbrain. This was most dramatic for a 5-bp insertion between the RARE and site D, resulting in almost complete loss of enhancer function. That this was due to a spacing effect, and not to the disruption of a cryptic transcription factor binding site or the allosteric effects of flanking residues on retinoid receptor binding (Oosterveen et al., 2003), was proved by the striking restoration of expression following extension of the insertion to 11 bp. The simplest interpretation of the combined results is that correct *Hoxd4* expression is dependent on stereospecific interactions between retinoid receptors and one or more transcription factors bound to sites D, E and F.

PAX6 and Hoxd4 enhancer function

We present multiple lines of evidence implicating PAX6 in the control of *Hoxd4* neural enhancer activity. PAX6 binds a sequence spanning sites D and E that shows some similarity to the established consensus. Significant divergence from the consensus is typical of PAX binding sites (Callaerts et al., 1997). Likewise the adjacent RARE in the *Hoxd4* neural enhancer differs from the DR5 consensus at one position, resulting in a 3-fold reduction in affinity for an RXRα●RARα heterodimer

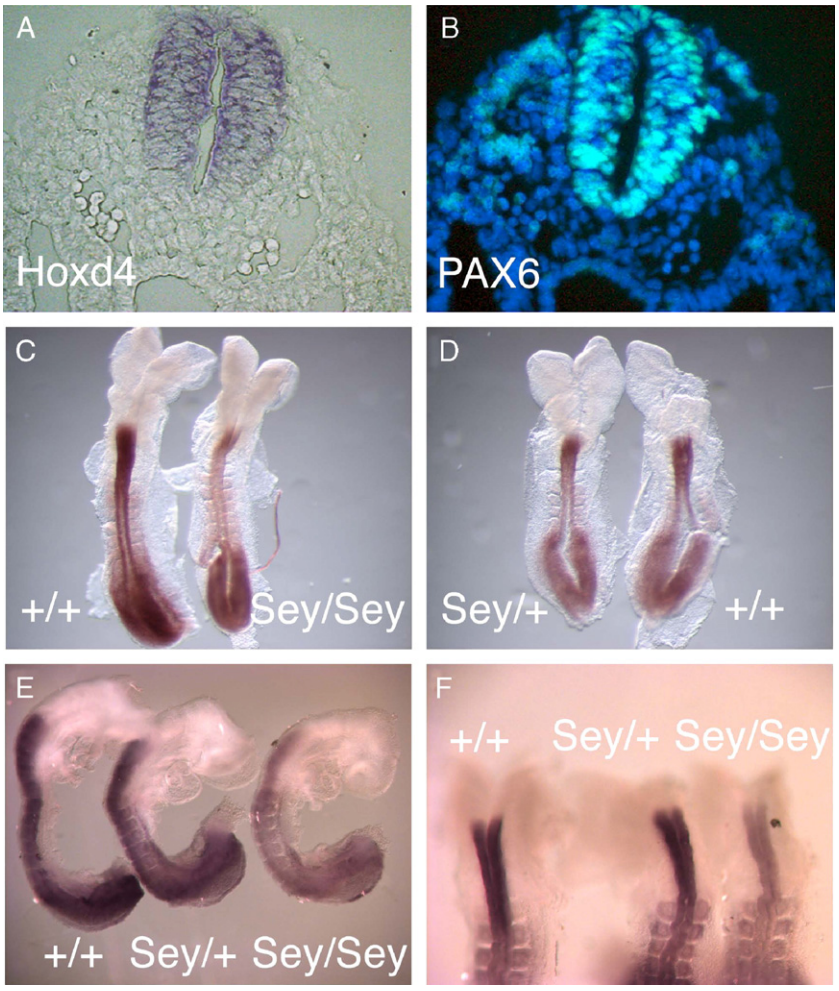

Fig. 6. *Hoxd4* expression is reduced in the neural tube of *Pax6* mutant embryos. (A) A wt E8.5 embryo probed for *Hoxd4* expression by whole-mount *in situ* hybridization was embedded and sectioned by cryostat. The section shown is at the level of the posterior hindbrain. (B) The same section was probed for PAX6 protein distribution across the DV axis using a 1:100 dilution of an anti-PAX6 C-terminal antibody (green). Nuclei in the same section were stained with DAPI (blue) and the two images superimposed. (C–F) Somite-matched littermates from crosses of Sey^{Neu} heterozygotes were examined in parallel for *Hoxd4* expression by whole-mount *in situ* hybridization. (C) *Hoxd4* expression is decreased in E8.5 Sey^{Neu} homozygotes (Sey/Sey) vs. wt (+/+). Embryos are at the 10- to 11-somite stage. (D) Comparable *Hoxd4* transcript levels in E8.0 Sey^{Neu} heterozygotes vs. wt. Embryos are at the 7-somite stage. (E, F) Lateral (E) and dorsal (F) views of *Hoxd4* expression in wt, heterozygous and homozygous Sey^{Neu} embryos at E8.75. Embryos are at the 12- to 13-somite stage.

(Mainguy et al., 2003; Nolte et al., 2003). Such non-optimal binding sites in natural regulatory regions are the norm, and may ensure that stable complexes of enhancer binding proteins are only formed when the full complement of factors are present to supply compensatory stabilizing protein-protein contacts. Such interactions should be stereospecific in many instances and would account for the spacing requirements noted here.

The PAX6CON, but not the P3 oligonucleotide, competed PAX6 binding in EMSA, implicating the PAX6 PD, but not the HD, in binding to region D–E. By comparison to the crystal structure of the PAX6 PD bound to an extended consensus (Xu et al., 1999), the N-terminal DNA binding domain of the PD (N subdomain) should contact site D of the *Hoxd4* neural enhancer, whereas the C-terminal DNA binding domain (C subdomain) should contact site E (Fig. 4A). The five-bp insertion between sites D and E would not alter nucleotides normally recognized by either N or C subdomain, but rather the region contacted by the extended polypeptide linker that joins these two DNA-binding structures (Xu et al., 1999). Mutation of site E and the 5-bp insertion between D and E evoke very similar alterations in transgene expression, both in terms of the extent of posteriorization and the altered DV profile of the retracted border. This would be most easily explained by a common disruption of DNA binding by the C subdomain of the protein, in one case due to the loss of site E, and in the other by preventing binding by both PD subdomains at once. The latter explanation also assumes that the physical constraints of the altered enhancer favor binding by the N subdomain to site D over that of the C subdomain to site E.

By contrast to other 5-bp insertions, that between sites E and F anteriorized transgene expression into r6, and greatly augmented ectopic expression in the area of the forebrain, eye, and olfactory epithelium, all tissues known to come under *Pax6* control (Callaerts et al., 1997). This result suggests a relaxation of negative regulatory controls, perhaps exercised through inhibitory factor(s) bound to site F and whose

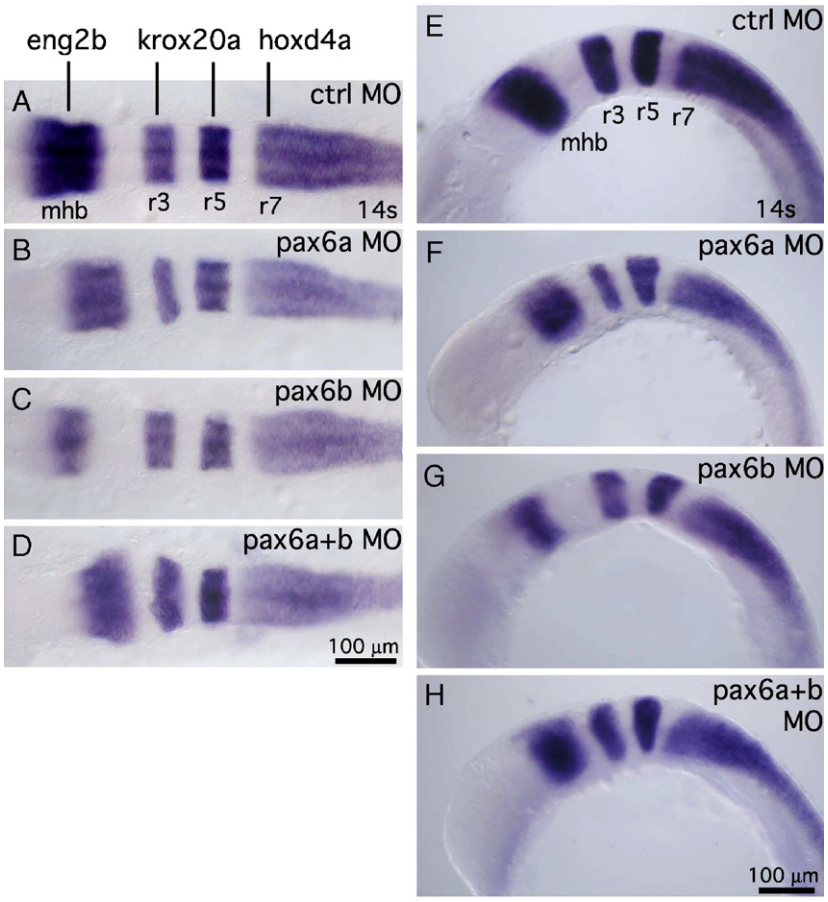

Fig. 7. Reduced pax6 function results in widespread AP patterning defects in the zebrafish hindbrain, and decreased and anteriorized *hoxd4a* expression. MOs against *pax6a* and *pax6b* were used to assess the effect of reduced Pax6 function on *hoxd4a* expression in the hindbrain of 14-somite embryos. Panels show dorsal (A–D) and lateral views (E–H) of embryos injected with one or both MOs and simultaneously probed for the expression of three genes, *eng2b*, *krox20a*, and *hoxd4a*. mhb, mid-hindbrain region. ctrl MO, control morpholino-substituted oligonucleotide.

interactions are disrupted by topological change. Conversely, the same mutation may reinforce interactions with adjacently bound PAX6.

While our findings demonstrate that PAX6 directly binds and regulates the *Hoxd4* neural enhancer, they provide no definitive proof that it is this factor which undergoes stereospecific interactions with the adjacently bound retinoid receptors. Nonetheless, adjacent binding sites for retinoid receptors and PAX6 have also been characterized in an enhancer of the chicken γE- and γF-crystallin genes (Králová et al., 2002), suggesting that these factors act in concert to regulate additional targets.

Early and late phases in the establishment Hoxd4 neural expression

Studies on another gene of paralogy group 4, *Hoxb4*, have defined distinct early and late neural enhancers (Gould et al., 1997, 1998). The early enhancer is dependent on a RARE orthologous to that which we have defined in *Hoxd4*, while the late enhancer harbors a pararegulatory element that binds paralogy group 4 HOX proteins and is sufficient to set the r6/7 border. While *Hoxd4* lacks this pararegulatory element, *Hoxd4* expression in Sey^{Neu} mice also follows early and late dynamics. Thus, at E8.5 and E8.75, *Hoxd4* transcript levels are depressed throughout the *Hoxd4* domain of Sey^{Neu} homozygotes (Fig. 6), but are restored by E11 (data not shown). Likewise, the altered *hoxd4a* anterior expression border following *pax6a* and *pax6b* MO injection is rescued later in development (data not shown). Thus, mechanisms governing *Hoxd4* expression at early and late times are distinct, as for *Hoxb4* (Gould et al., 1998), and consistent with other studies on *Hoxd4* (Maves and Kimmel, 2005). This observation correlates well with our finding that PAX6 is only associated with the *Hoxd4* enhancer in posterior embryonic tissue on E8, but not on E10. Thus, at both the molecular and genetic levels, *Pax6* distinguishes early from late *Hoxd4* neural enhancer function. Our previous work showed that hours before *Hoxd4* transcripts are detectable in the E8 mouse embryo, histones at the neural enhancer have acquired the acetylation and methylation signatures of transcriptionally active chromatin, and the histone acetyltransferase (HAT) CREB binding protein (CBP) has been recruited (Rastegar et al., 2004). Chromatin thus anticipates gene activation at the *Hoxd4* enhancer. The molecular and genetic evidence presented here suggests that PAX6, along with retinoid receptors, is responsible for these early changes, supported

by observations that both transcription factors recruit CBP/p300 (Hussain and Habener, 1999; Weston et al., 2003).

Evolutionary conservation of the intersection of AP and DV patterning systems

A surprising implication of our studies is that PAX6, a protein known for its key role in DV patterning of the CNS, also contributes to the setting of the *Hoxd4* anterior expression border. In fact, down-regulation of *pax6a* and *pax6b* generates widespread AP patterning defects within rhombomeres (Figs. 7E–H), suggesting a broad role for Pax6 in hindbrain morphogenesis along the vertebrate rostro-caudal axis. RA also directs both AP and DV patterning (Wilson and Maden, 2005), providing Hoxd4, and perhaps Hox genes generally, with the means to integrate positional cues from the same two classes of transcription factor (retinoid receptors and PAX6) for precise spatio-temporal activation across the AP and DV axes of the neural tube.

Previous studies have demonstrated the integration of AP and DV positional cues in the elaboration of neural-specific gene expression patterns and neuronal cell type (Dasen et al., 2003; Gaufo et al., 2004; Pattyn et al., 2003; Samad et al., 2004; Wilson et al., 2004; Wilson and Maden, 2005). Evidence that AP and DV patterning mechanisms are likely to be cross-referenced at additional levels is given by the demonstration that HOX-containing complexes influence the neural-specific expression of *Pax3* (Pruitt et al., 2004). The selective advantage to reciprocal control by distinct axial patterning systems could arise from increased precision in setting expression/compartment borders in time and space. For example, DV signals could restrict *Hox* expression to appropriate positions along this axis (Krieger et al., 2004). Thus, many more instances of reciprocal AP–DV regulatory interactions can be expected.

Acknowledgments

Sincere thanks to Simon Saule for the generous gift of anti-PAX6 antibodies, Michael German for the *Pax6* expression constructs, Yosé Chateauvert, Annette Neubüser and Yingzi Yue for helping with the Sey^{Neu} strain and additional mouse work, Amber Starks for helping with the morpholino injections, and Nathalie Perreault for the helpful discussions. M.R. was supported by a CIHR Cancer Consortium Training Grant Fellowship Award from the McGill Cancer Centre, and by a Conrad F. Harrington Fellowship Award from the Faculty of Medicine, McGill University. M.B. holds a Canada Research Chair in Kidney Disease. M.F. is a Chercheur-National of the Fonds de la Recherche en Santé du Québec. This work was supported by grants P01HD22486 and R01RR10715 from the National Institutes of Health (USA) to J.H.P., and from the Canadian Institutes of Health Research (CIHR) grant #67219 to M.B. and CIHR grant #49498 to M.F.

Appendix A. Supplementary data

Supplementary data associated with this article can be found, in the online version, at doi:10.1016/j.ydbio.2006.08.061.

References

Callaerts, P., Halder, G., Gehring, W.J., 1997. PAX-6 in development and evolution. Annu. Rev. Neurosci. 20, 483–532.

Chi, N., Epstein, J.A., 2002. Getting your Pax straight: Pax proteins in development and disease. Trends Genet. 18, 41–47.

Cvekl, A., Sax, C.M., Bresnick, E.H., Piatigorsky, J., 1994. A complex array of positive and negative elements regulates the chicken alpha A-crystallin gene: involvement of Pax-6, USF, CREB and/or CREM, and AP-1 proteins. Mol. Cell. Biol. 14, 7363–7376.

Cvekl, A., Kashanchi, F., Sax, C.M., Brady, J.N., Piatigorsky, J., 1995. Transcriptional regulation of the mouse alpha A-crystallin gene: activation dependent on a cyclic AMP-responsive element (DE1/CRE) and a Pax-6-binding site. Mol. Cell. Biol. 15, 653–660.

Daniels, E., Letourneau, S., Turbide, C., Kuprina, N., Rudinskaya, T., Yazova, A.C., Holmes, K.V., Dveksler, G.S., Beauchemin, N., 1996. Biliary glycoprotein 1 expression during embryogenesis: correlation with events of epithelial differentiation, mesenchymal-epithelial interactions, absorption, and myogenesis. Dev. Dyn. 206, 272–290.

Dasen, J.S., Liu, J.P., Jessell, T.M., 2003. Motor neuron columnar fate imposed by sequential phases of Hox-c activity. Nature 425, 926–933.

Deschamps, J., van Nes, J., 2005. Developmental regulation of the Hox genes during axial morphogenesis in the mouse. Development 132, 2931–2942.

Draper, B.W., Morcos, P.A., Kimmel, C.B., 2001. Inhibition of zebrafish fgf8 pre-mRNA splicing with morpholino oligos: a quantifiable method for gene knockdown. Genesis 30, 154–156.

Ekker, M., Wegner, J., Akimenko, M.A., Westerfield, M., 1992. Coordinate embryonic expression of three zebrafish engrailed genes. Development 116, 1001–1010.

Epstein, J., Cai, J., Glaser, T., Jepeal, L., Maas, R., 1994. Identification of a Pax paired domain recognition sequence and evidence for DNA-dependent conformational changes. J. Biol. Chem. 269, 8355–8361.

Ericson, J., Rashbass, P., Schedl, A., Brenner-Morton, S., Kawakami, A., van Heyningen, V., Jessell, T.M., Briscoe, J., 1997. Pax6 controls progenitor cell identity and neuronal fate in response to graded Shh signaling. Cell 90, 169–180.

Featherstone, M., 2003. Hox proteins and their co-factors in transcriptional regulation. In: Lufkin, T. (Ed.), Murine Homeobox Gene Control of Embryonic Patterning and Organogenesis, vol. 13. Elsevier, Amsterdam, pp. 1–42.

Featherstone, M.S., Baron, A., Gaunt, S.J., Mattei, M.-G., Duboule, D., 1988. Hox-5.1 defines a homeobox-containing gene locus on mouse chromosome 2. Proc. Natl. Acad. Sci. U. S. A. 85, 4760–4764.

Folberg, A., Nagy Kovács, E., Featherstone, M.S., 1997. Characterization and retinoic acid responsiveness of the murine Hoxd4 transcription unit. J. Biol. Chem. 272, 29151–29157.

Gaufo, G.O., Wu, S., Capecchi, M.R., 2004. Contribution of Hox genes to the diversity of the hindbrain sensory system. Development 131, 1259–1266.

Gaunt, S.J., Krumlauf, R., Duboule, D., 1989. Mouse homeogenes within a subfamily, Hox-1.4, -2.6 and -5.1, display similar anteroposterior domains of expression in the embryo, but show stage- and tissue-dependent differences in their regulation. Development 107, 131–141.

Gavalas, A., Krumlauf, R., 2000. Retinoid signalling and hindbrain patterning. Curr. Opin. Genet. Dev. 10, 380–386.

Gould, A., Morrison, A., Sproat, G., White, R.A.H., Krumlauf, R., 1997. Positive cross-regulation and enhancer sharing—two mechanisms for specifying overlapping Hox expression patterns. Genes Dev. 11, 900–913.

Gould, A., Itasaki, N., Krumlauf, R., 1998. Initiation of rhombomeric Hoxb4 expression requires induction by somites and a retinoid pathway. Neuron 21, 39–51.

Haller, K., Rambaldi, I., Daniels, E., Nagy Kovács, E., Featherstone, M., 2002. *Prep2*, cloning and expression of a new *Prep* family member. Dev. Dyn. 225, 358–364.

Henrique, D., Adam, J., Myat, A., Chitnis, A., Lewis, J., Ish-Horowicz, D., 1995. Expression of a Delta homologue in prospective neurons in the chick. Nature 375, 787–790.

Hill, R.E., Favor, J., Hogan, B.L., Ton, C.C., Saunders, G.F., Hanson, I.M., Prosser, J., Jordan, T., Hastie, N.D., van Heyningen, V., 1991. Mouse small eye results from mutations in a paired-like homeobox-containing gene. Nature 354, 522–525.

Ho, S.N., Hunt, H.D., Horton, R.M., Pullen, J.K., Pease, L.R., 1989. Site-directed mutagenesis by overlap extension using the polymerase chain reaction. Gene 77, 51–59.

Hogan, B., Beddington, R., Costantini, F., Lacy, E., 1994. Manipulating the Mouse Embryo: A Laboratory Manual. Cold Spring Harbor Laboratory Press.

Hombria, J.C., Lovegrove, B., 2003. Beyond homeosis—HOX function in morphogenesis and organogenesis. Differentiation 71, 461–476.

Hussain, M.A., Habener, J.F., 1999. Glucagon gene transcription activation mediated by synergistic interactions of pax-6 and cdx-2 with the p300 co-activator. J. Biol. Chem. 274, 28950–28957.

Jowett, T., Yan, Y.L., 1996. Double fluorescent in situ hybridization to zebrafish embryos. Trends Genet. 12, 387–389.

Králová, J., Czerny, T., Spanielová, H., Ratajová, V., Kozmik, Z., 2002. Complex regulatory element within the gammaE- and gammaF-crystallin enhancers mediates Pax6 regulation and is required for induction by retinoic acid. Gene 286, 271–282.

Krieger, K.E., Abbott, M.A., Joksimovic, M., Lueth, P.A., Sonea, I.M., Jeannotte, L., Tuggle, C.K., 2004. Transgenic mice ectopically expressing HOXA5 in the dorsal spinal cord show structural defects of the cervical spinal cord along with sensory and motor defects of the forelimb. Brain Res. Dev. Brain Res. 150, 125–139.

Krumlauf, R., 1994. Hox genes in vertebrate development. Cell 78, 191–201.

Mainguy, G., In der Rieden, P.M., Berezikov, E., Woltering, J.M., Plasterk, R.H., Durston, A.J., 2003. A position-dependent organisation of retinoid response elements is conserved in the vertebrate Hox clusters. Trends Genet. 19, 476–479.

Maves, L., Kimmel, C.B., 2005. Dynamic and sequential patterning of the zebrafish posterior hindbrain by retinoic acid. Dev. Biol. 285, 593–605.

Morrison, A., Ariza-McNaughton, L., Gould, A., Featherstone, M., Krumlauf, R., 1997. HOXD4 and regulation of the group 4 paralog genes. Development 124, 3135–3146.

Nolte, C., Amores, A., Nagy Kovacs, E., Postlethwait, J., Featherstone, M., 2003. The role of a retinoic acid response element in establishing the anterior neural expression border of Hoxd4 transgenes. Mech. Dev. 120, 325–335.

Oosterveen, T., van Vliet, P., Deschamps, J., Meijlink, F., 2003. The direct context of a hox retinoic acid response element is crucial for its activity. J. Biol. Chem. 278, 24103–24107.

Osumi, N., Hirota, A., Ohuchi, H., Nakafuku, M., Iimura, T., Kuratani, S., Fujiwara, M., Noji, S., Eto, K., 1997. Pax-6 is involved in the specification of hindbrain motor neuron subtype. Development 124, 2961–2972.

Oxtoby, E., Jowett, T., 1993. Cloning of the zebrafish krox-20 gene (krx-20) and its expression during hindbrain development. Nucleic Acids Res. 21, 1087–1095.

Pattyn, A., Vallstedt, A., Dias, J.M., Samad, O.A., Krumlauf, R., Rijli, F.M., Brunet, J.F., Ericson, J., 2003. Coordinated temporal and spatial control of motor neuron and serotonergic neuron generation from a common pool of CNS progenitors. Genes Dev. 17, 729–737.

Phelan, M.L., Rambaldi, I., Featherstone, M.S., 1995. Cooperative interactions between HOX and PBX proteins mediated by a conserved peptide motif. Mol. Cell. Biol. 15, 3989–3997.

Prince, V.E., Joly, L., Ekker, M., Ho, R.K., 1998. Zebrafish hox genes: genomic organization and modified colinear expression patterns in the trunk. Development 125, 407–420.

Pruitt, S.C., Bussman, A., Maslov, A.Y., Natoli, T.A., Heinaman, R., 2004. Hox/Pbx and Brn binding sites mediate Pax3 expression in vitro and in vivo. Gene Expression Patterns 4, 671–685.

Püschel, A.W., Gruss, P., Westerfield, M., 1992. Sequence and expression pattern of pax-6 are highly conserved between zebrafish and mice. Development 114, 643–651.

Rastegar, M., Kobrossy, L., Kovacs, E.N., Rambaldi, I., Featherstone, M., 2004. Sequential histone modifications at Hoxd4 regulatory regions distinguish anterior from posterior embryonic compartments. Mol. Cell. Biol. 24, 8090–8103.

Samad, O.A., Geisen, M.J., Caronia, G., Varlet, I., Zappavigna, V., Ericson, J., Goridis, C., Rijli, F.M., 2004. Integration of anteroposterior and dorsoventral regulation of Phox2b transcription in cranial motoneuron progenitors by homeodomain proteins. Development 131, 4071–4083.

Simpson, T.I., Price, D.J., 2002. Pax6; a pleiotropic player in development. BioEssays 24, 1041–1051.

Suzuki, M., Mizutani-Koseki, Y., Fujimura, Y., Miyagishima, H., Kaneko, T., Takada, Y., Akasaka, T., Tanzawa, H., Takihara, Y., Nakano, M., Masumoto, H., Vidal, M., Isono, K., Koseki, H., 2002. Involvement of the Polycomb-group gene Ring1B in the specification of the anterior–posterior axis in mice. Development 129, 4171–4183.

Tagle, D.A., Koop, B.F., Goodman, M., Slightom, J.L., Hess, D.L., Jones, R.T., 1988. Embryonic epsilon and gamma globin genes of a prosimian primate (*Galago crassicaudatus*). Nucleotide and amino acid sequences, developmental regulation and phylogenetic footprints. J. Mol. Biol. 203, 439–455.

Takahashi, K., Vigneron, M., Matthes, H., Wildeman, A., Zenke, M., Chambon, P., 1986. Requirement of stereospecific alignments for initiation from the simian virus 40 early promoter. Nature 319, 121–126.

Turque, N., Plaza, S., Radvanyi, F., Carriere, C., Saule, S., 1994. Pax-QNR/Pax-6, a paired box- and homeobox-containing gene expressed in neurons, is also expressed in pancreatic endocrine cells. Mol. Endocrinol. 8, 929–938.

Underhill, D.A., 2000. Genetic and biochemical diversity in the Pax gene family. Biochem. Cell Biol. 78, 629–638.

Walther, C., Gruss, P., 1991. Pax-6, a murine paired box gene, is expressed in the developing CNS. Development 113, 1435–1449.

Weston, A.D., Blumberg, B., Underhill, T.M., 2003. Active repression by unliganded retinoid receptors in development: less is sometimes more. J. Cell Biol. 161, 223–228.

Wilson, L., Maden, M., 2005. The mechanisms of dorsoventral patterning in the vertebrate neural tube. Dev. Biol. 282, 1–13.

Wilson, D.S., Guenther, B., Desplan, C., Kuriyan, J., 1995. High resolution crystal structure of a paired (Pax) class cooperative homeodomain dimer. Cell 82, 709–719.

Wilson, L., Gale, E., Chambers, D., Maden, M., 2004. Retinoic acid and the control of dorsoventral patterning in the avian spinal cord. Dev. Biol. 269, 433–446.

Xu, P.X., Woo, I., Her, H., Beier, D.R., Maas, R.L., 1997. Mouse Eya homologues of the *Drosophila* eyes absent gene require Pax6 for expression in lens and nasal placode. Development 124, 219–231.

Xu, H.E., Rould, M.A., Xu, W., Epstein, J.A., Maas, R.L., Pabo, C.O., 1999. Crystal structure of the human Pax6 paired domain-DNA complex reveals specific roles for the linker region and carboxy-terminal subdomain in DNA binding. Genes Dev. 13, 1263–1275.

Zhang, F., Pöpperl, H., Morrison, A., Nagy Kovács, E., Schwarz, L., Prideaux, V., Krumlauf, R., Rossant, J., Featherstone, M.S., 1997. Elements both 5′ and 3′ to the murine Hoxd4 gene establish anterior borders of expression in mesoderm and neurectoderm. Mech. Dev. 67, 49–58.

Zhang, F., Kovács, E.N., Featherstone, M.S., 2000. Murine Hoxd4 expression in the CNS requires multiple elements including a retinoic acid response element. Mech. Dev. 96, 79–89.